Available online at http://scik.org
Commun. Math. Biol. Neurosci. 2022, 2022:115
https://doi.org/10.28919/cmbn/7734
ISSN: 2052-2541

COVID-19 SPATIOTEMPORAL SIR MODEL: REGIONAL OPTIMAL CONTROL APPROACH

MAROUANE KARIM*, SOUKAINA BEN RHILA, HAMZA BOUTAYEB, MOSTAFA RACHIK

Laboratory of Analysis Modeling and Simulation, Department of Mathematics and Computer Science, Faculty of Sciences Ben M'Sik, Hassan II University Casablanca, BP 7955, Sidi Othman, Casablanca, Morocco

Abstract. In the present work, we consider a spatio-temporal model to describe the evolution of covid19 in an area Ω (Ω can be a city, a country,..). Taking into account the financial means of the considered country, we suppose that the number of available vaccines is destined to a region $\omega_1 \subseteq \Omega$ (ω_1 can be an industrial city, a university city. ..) and we suppose that the available treatments are dedicated to a region $\omega_2 \subseteq \Omega$ (ω_2 can be a military city,..), it is not excluded that $\omega_1 = \omega_2$. To minimize the number of infection with minimal cost, we apply an optimal regional control strategy to stop the death of infected individuals in the considered area. Much of this work has been devoted to mathematical study, where the existence of the optimal controls and the solutions of the state system are proven, an optimal control characterization in terms of state and adjoint functions are provided, and the optimality system is solved numerically using a forward-backward sweep method. Our numerical results suggest that when vaccination and treatment procedures are used together, the control approach becomes more effective in protecting a specific region from epidemic transmission from neighboring regions.

Keywords: spatial-temporal transmission; Covid-19; regional optimal control; numerical method.

2010 AMS Subject Classification: 92C60.

*Corresponding author

E-mail address: karim.marouane00@gmail.com

Received September 12, 2022

1. INTRODUCTION

Mathematical modeling in epidemiology is a pertinent instrument for public health decision makers. In principle, public policy considerations should be supported by experiments that can directly measure the impact of public health measures, but for operational purposes, such experiments are not always feasible. This is where the contribution of mathematical modelling to the evaluation and anticipation of the effects of public health programs is significant. The first mathematical models that describe an infectious illness date back to Bernouilli [1, 2] in 1766. In 1911, Sir Ronald Ross [3] provided the first mathematical model of malaria transmission. In 1927, W.O. Kermak and A.G. McKendrick applied the ideas of Ronald Ross to the studies of the transmission dynamics of human infectious diseases. More particularly, Kermack and Mckendrick applied Ross' ideas to diseases whose transmission dynamics were dependent on the frequency and intensity of interactions between susceptible and infectious individuals. Their results [4], published in 1927, continue to hold a central role in the mathematical analysis of infectious diseases. Recently, several diseases have been modeled using the SIR model [5, 6, 7, 8]. Nevertheless, in the last models, it was often assumed that the distribution of the population was homogeneous in the study space, which does not represent the truth, as we can see in the cities or countries where we live. This is not the case. There are areas of low, medium, and high density, so we cannot say that a person living in a low-density area will have the same number of meetings as a person living in a high-density area, for example. This observation made it possible to introduce spatial behavior into the SIR epidemiological model by including the diffusion term in these different compartments, which involves that the population is dispersed over a spatial region and that it requires time for an infection to propagate within this region [9, 10].

Nowadays, the whole world is aware of one of the most dangerous pandemics that humanity has ever witnessed. The Coronavirus, or the so-called COVID-19 pandemic, started in Wuhan, the Chinese city, in early December 2019. Since its appearance, it has created a state of panic and terror among all different countries worldwide, and caused the deaths of millions of people on this planet, triggering global severe social and economic damage, including the largest global economic recession since the great depression, and the postponement or cancellation

of sporting, religious, political, and cultural events. Significant shortages of supplies and equipment were exacerbated by panic buying, and schools, universities, as well as colleges were closed at national or local levels in 190 countries, affecting about 73.5% of students all over the world [11, 12, 13]. By direct contact, the virus can be transmitted from an infected person to others by shaking hands and touching contaminated surfaces. As a consequence, the infection affects different organs in the human body, such as the eyes, nose, and mouth. The outbreak appeared first in Wuhan, then spread to all Chinese provinces. Cases have also been reported in many other Asian and European states, as people move, possibly carrying Covid-19 to intercontinental destinations and so far from Wuhan to the United States and Canada, so as to spread around the world at a breakneck speed. In addition, the World Health Organization (WHO) officially announced on January 30 that the virus outbreak was a public health emergency of international concern [14] and confirmed that the outbreak turned into a pandemic on March 11.

The control of epidemics is of increasing importance to governments and public health officials. Specifically, the goal is to understand the spatial dynamics of the spread of infectious diseases in order to develop prevention and intervention strategies to reduce their impact on the population. It is hoped that the interaction of spatial factors in mathematical models of infectious diseases will lead to a better understanding, prediction, and control of this movement behavior. Thus, there is no need to justify the critical importance of spatial dynamics in the description and analysis of infectious diseases. In comparison, few focus on the spatio-temporal pattern, a related and important concept in mathematical epidemiological models. Because of the movement of thousands of people from one region to another, the existence of a spatial component has a remarkable probability. In this case, an epidemic can spread rapidly over a large area regardless of borders. The geographic scale is therefore central to a multitude of studies of diseases, which become spatially mobile in different regions by moving from one area to another.

According to numerous research studies taking into account the spatial aspect of an epidemic spread [15, 16, 17], we study an extension of the basic SIR model, in which we integrate the spatial behavior of the population and two terms of control strategies, representing the

vaccination and the treatment program. The main motivation is to work on the effect of the treatment and vaccination program on the spread of COVID-19 in a specific area in order to minimize the number of infected individuals and to reduce the cost of our controls. Therefore, this work is committed to the mathematical study of the existence and characterization of spatiotemporal optimal control that minimizes the density of the infected people, the cost of the treatment, and the vaccination program. It is important to note here that our work is distinguished from some other associated studies cited in this article, such as [18, 19, 20, 21] because our work uses two distributional controls that represent the percentage of susceptible and infected individuals vaccinated and treated respectively for the SIR diffusion reaction system.

The structure of this work is the following; Section 2 is staunched to the basic mathematical model and the associated optimal control problem. Section 3, we demonstrate the existence of a global strong solution for our system. In section 4, we prove the existence of an optimal solution. Neccesary optimality conditions are confirmed in section 5. As application, the numerical results related to our control problem are given in section 6. In the end, we conclude the article in section 7.

2. The Basic Mathematical Model

2.1. The model without controls. Most of the work in modeling the dynamics of viral diseases has used SIR models to understand and predict their spread [22, 23]. In this work, we formulate an optimal control problem based on a spatiotemporal epidemic model. We presume that the population habitat is a spatially heterogeneous environment, where the residents show a tendency to move to regions and their densities will be conditional on space. We give an extension of these models by introducing the spatial behavior of the population by adding the term of spatial diffusion. We write $S(t,x)$, $I(t,x)$ and $R(t,x)$ to indicate that the populations have spatial and temporal behavior for the susceptible population density, infected population density and removed population density, respectively. The time t belongs to a finite interval $[0,T]$, while x varies in a bounded domain $\Omega \subseteq \mathbb{R}^2$. The population dynamics is given by the following system

$$(1)\qquad \begin{cases} \dfrac{\partial S}{\partial t} = \Lambda + \lambda\Delta S - bSI - mS \\ \dfrac{\partial I}{\partial t} = \beta\Delta I + bSI - (g+m+k)\,I \qquad (t,x) \in Q = [0,T]\times\Omega \\ \dfrac{\partial R}{\partial t} = \gamma\Delta R + gI - mR \end{cases}$$

with the homogenous Neumann boundary conditions

$$(2)\qquad \frac{\partial S}{\partial \eta} = \frac{\partial R}{\partial \eta} = \frac{\partial I}{\partial \eta} = 0, \quad (t,x) \in \Sigma = [0,T]\times\partial\Omega$$

where $\dfrac{\partial}{\partial \eta}$ is the outward normal derivative, Λ is the birth rate, b is the effective contact rate, m is the natural mortality rate, g is the recovery rate, k is the induced death rate of Covid-19. λ, β and γ are the self-diffusion coefficients for the susceptible, infected and removed individuals. The initial distribution of the three populations is supposed to be

$$(3)\qquad S(0,x) = S_0 \geq 0,\ R(0,x) = R_0 \geq 0 \text{ and } I(0,x) = I_0 \geq 0$$

2.2. The model with controls. As a strategy of control, we adopt a regional treatment program, so into the model (1), we include two controls $u(.)\chi_{\omega_1}(.)$ and $v(.)\chi_{\omega_2}(.)$ where $u(.)$ and $v(.) \in L^2(0,T;\mathbb{R})$ and χ_ω is the characteristic function of ω. The control $u\chi_{\omega_1}$ represents the percentage of the sensible that is vaccinated per unit of time in the region ω_1 while the controle $v\chi_{\omega_2}$ represents the percentage of the treated infections per time in the region ω_2. The two controls represent the effect of the therapeutic treatment applied to the infected and susceptible persons who act in the subdomains $\omega_1, \omega_2 \subset \Omega$. The dynamic of the regional controlled system is given by

$$(4)\qquad \begin{cases} \dfrac{\partial S}{\partial t} = \Lambda + \lambda\Delta S - bSI - mS - u\chi_{\omega_1}(x)S \\ \dfrac{\partial I}{\partial t} = \beta\Delta I + bSI - (g+m+k)\,I - v\chi_{\omega_2}(x)I \qquad (t,x) \in Q = [0,T]\times\Omega \\ \dfrac{\partial R}{\partial t} = \gamma\Delta R + gI - mR + v\chi_{\omega_2}(x)I + u\chi_{\omega_1}(x)S \end{cases}$$

$$(5)\qquad \frac{\partial S}{\partial \eta} = \frac{\partial R}{\partial \eta} = \frac{\partial I}{\partial \eta} = 0, \quad (t,x) \in \Sigma = [0,T]\times\partial\Omega$$

$$S(0,x) = S_0 \geq 0,\ R(0,x) = R_0 \geq 0 \text{ and } I(0,x) = I_0 \geq 0,\ \ x \in \Omega \tag{6}$$

Our goal is to minimize the density of infected individuals also to maximize the removed ones in both regions ω_1 and ω_2, and also to reduce the cost of treatment program. Mathematically, our problem is to minimize the objective functional

$$J((S,I,R),u,v) = \|I\|^2_{L^2(Q)} - \|R\|^2_{L^2(Q)} + \frac{\rho}{2}(\|u\|^2_{L^2([0,T]\times\omega_1)} + \|v\|^2_{L^2([0,T]\times\omega_2)}) \tag{7}$$

under the control set U_{ad} defined by

$$U_{ad} = \left\{(u\chi_{\omega_1}, v\chi_{\omega_2}) \in (L^2([0,T]\times L^2(\Omega)))^2;\ 0 \leq u \leq 1 \, and \, 0 \leq v \leq 1\right\} \tag{8}$$

and where ρ is a positive weight associated with the control. Indeed, let's consider

- $W^{1,2}([0,T];H(\Omega))$ the space of all absolutely continuous functions $f : [0,T] \longmapsto H(\Omega)$ having the property that $\dfrac{\partial f}{\partial t} \in W^{1,2}([0,T];H(\Omega))$ where $H(\Omega) = \left(L^2(\Omega)\right)^3$.
- $L(T,\Omega) = L^2\left(0,T;H^2(\Omega)\right) \cap L^\infty\left(0,T;H^1(\Omega)\right)$

3. Existence of Global Solution

We study in this section the existence of a (global) strong solution, of system (4-6), as our mathematical model is related to a population evolution, then for biological reasons, the populations S, I and R should remain non-negative and bounded.

Let $c = (c_1,c_2,c_3) = (S,I,R)$ the solution of the system (4-6) with $c^0 = (S_0,I_0,R_0) = \left(c_1^0,c_2^0,c_3^0\right)$. Denote by A the linear operator defined as follow

$$\begin{gathered} A : D(A) \subset H(\Omega) \longrightarrow H(\Omega) \\ Ac = (\lambda\Delta c_1, \beta\Delta c_2, \gamma\Delta c_3) \in D(A), \forall c \in D(A) \end{gathered} \tag{9}$$

$$D(A) = \left\{c \in \left(H^2(\Omega)\right)^3, \frac{\partial c_1}{\partial \eta} = \frac{\partial c_2}{\partial \eta} = \frac{\partial c_3}{\partial \eta} = 0, a.e \in \partial\Omega\right\} \tag{10}$$

Theorem 1. *Let Ω be a bounded domain from $\mathbb{R}^2$, with the boundary of class $C^{2+\alpha}$,$\alpha > 0$. As the rates $b,m,g,k > 0$, $(u,v) \in U_{ad}$, $c^0 \in D(A)$ and $c_i^0 \geq 0$ on Ω (for $i = 1,2,3$), the system*

(4–6) has a unique (global) strong solution $c \in W^{1,2}([0,T];H(\Omega))$ *such that*

$$c_1, c_2, c_3 \in L(T,\Omega) \cap L^{\infty}(Q)$$

In addition, there exists $\Gamma > 0$ *independent of* (u,v) *(and of the corresponding solution c) such that for a* $t \in [0,T]$

$$\left\| \frac{\partial c_i}{\partial t} \right\|_{L^2(Q)} + \|c_i\|_{L^2\left(0,T,H^2(\Omega)\right)} + \|c_i\|_{H^1(\Omega)} + \|c_i\|_{L^{\infty}(Q)} \leq \Gamma, \text{for } i = 1,2,3 \tag{11}$$

Proof. For the proof of the existence of a (global) strong solution for system (4-6), let

$$\begin{cases} f_1(c(t)) = \Lambda - bc_1c_2 - mc_1 - u\chi_{\omega_1}(x)c_1 \\ f_2(c(t)) = bc_1c_2 - (g+m+k)c_2 - v\chi_{\omega_2}(x)c_2 \qquad t \in [0,T] \\ f_3(c(t)) = gc_2 - mc_3 + v\chi_{\omega_2}(x)c_2 + u\chi_{\omega_1}(x)c_1 \end{cases} \tag{12}$$

The nonlinear term in (12) and we consider the function $f(c(t)) = (f_1(c(t)), f_2(c(t), f_3(c(t))))$, then we can be rewritten the system (4-6) in the space $H(\Omega)$ under the form

$$\begin{cases} \dfrac{\partial c}{\partial t} = Ac + f(c(t)), \qquad t \in [0,T] \\ c(0) = c^0 \end{cases}$$

As the operator A defined in (9-10) is dissipating and self-adjoint and generates a C_0-semigroup of contractions on $H(\Omega)$ see [24] and [25], since $|c_i| \leq N \, for i = 1,2,3$ where N is a constant, that represents the total population. Thus function $f = (f_1, f_2, f_3)$ becomes Lipschitz continuous in $c = (c_1, c_2, c_3)$ uniformly with respect to $t \in [0,T]$, problem (4-6) admits a unique strong solution $c = (c_1, c_2, c_3) \in W^{1,2}([0,T];H(\Omega))$ (See [26, 27]), with $c_1, c_2, c_3 \in L^2\left(0,T;H^2(\Omega)\right)$.

In order to prove that $c \in L^{\infty}(Q)$, we put $M = \max\left\{ \|f_i\|_{L^{\infty}(Q)}, \left\|c_i^0\right\|_{L^{\infty}(\Omega)} \, for i = 1,2,3 \right\}$, it is obvious to see that the function $V_1(t,x) = c_1 - Mt - \left\|c_1^0\right\|_{L^{\infty}(\Omega)}$ satisfies the system

$$\begin{aligned} \frac{\partial V_1}{\partial t}(t,x) &= \lambda \triangle V_1 + f_1(t,c(t)) - M \quad t \in [0,T] \\ V_1(0,x) &= c_1^0 - \left\|c_1^0\right\|_{L^{\infty}(\Omega)} \end{aligned} \tag{13}$$

The solution of this system can be written

$$V_1(t) = S(t)\left(c_1^0 - \|c_1\|_{L^{\infty}(\Omega)}\right) + \int_0^t S(t-s)\left(f_1(c(s)) - M\right) ds,$$

with $\{S(t), t \geq 0\}$ is the C_0-semi-group generated by the operator $\bar{A} : D(B) \subset L^2(\Omega) \longrightarrow L^2(\Omega)$ where $\bar{A}u = \lambda \Delta c_1$ and $D(\bar{A}) = \left\{ c_1 \in H^2(\Omega), \frac{\partial c_1}{\partial \eta} = 0, a.e\, \partial\Omega \right\}$. Since $c_1^0 - \left\| c_1^0 \right\|_{L^\infty(\Omega)} \leq 0$ and $f_1(c(s)) - M \leq 0$, it follows that $V_1(t,x) \leq 0, \forall (t,x) \in Q$.

According to the same manner we can prove that the function $V_2(t,x) = c_1 + Mt + \left\| c_1^0 \right\|_{L^\infty(\Omega)}$ is nonnegative. Then $|c_1(t,x)| \leq Mt + \left\| c_1^0 \right\|_{L^\infty(\Omega)} \forall (t,x) \in Q$ and analogously

$$|c_i(t,x)| \leq Mt + \left\| c_i^0 \right\|_{L^\infty(\Omega)} \forall (t,x) \in Q \qquad for\ i = 2,3 \tag{14}$$

Thus, we have proved that $c_i \in L^\infty(\Omega)\ \forall (t,x) \in Q$ for $i = 1,2,3$.

By the first equation of (4) one obtains

$$\begin{aligned} &\int_0^t \int_\Omega \left| \tfrac{\partial c_1}{\partial t} \right|^2 dsdx + \lambda^2 \int_0^t \int_\Omega |\triangle c_1|^2 dsdx - 2\lambda \int_0^t \int_\Omega \tfrac{\partial c_1}{\partial t} \triangle c_1 dsdx \\ &\qquad = \int_0^t \int_\Omega (\Lambda - bc_1c_2 - mc_1 - u\chi_{\omega_1}(x)c_1)^2 dsdx \end{aligned}$$

Using the regularity of c_1 and the Greens formula, we can write

$$2\lambda \int_0^t \int_\Omega \tfrac{\partial c_1}{\partial t} \triangle c_1 dsdx \;=\; \lambda \int_\Omega |\nabla c_1|^2 dx - \lambda \int_\Omega \left| \nabla c_1^0 \right|^2 dx$$

Then

$$\begin{aligned} &\int_0^t \int_\Omega \left| \tfrac{\partial c_1}{\partial t} \right|^2 dsdx + \lambda^2 \int_0^t \int_\Omega |\triangle c_1|^2 dsdx + \lambda \int_\Omega |\nabla c_1|^2 dx - \lambda \int_\Omega \left| \nabla c_1^0 \right|^2 dx \\ &\qquad = \int_0^t \int_\Omega (\Lambda - bc_1c_2 - mc_1 - u\chi_{\omega_1}(x)c_1)^2 dsdx \end{aligned}$$

Since $c_i^0 \in H^2(\Omega)$ and $\|c_i\|_{L^\infty(Q)}$for $i = 1,2,3$ are bounded independently of v and u, we submit that $c_1 \in L^\infty\left(0,T,H^1(\Omega)\right)$ and the first inequality in (14) holds for $i = 1$. The remaining cases can be treated similarly.

Let show the positiveness of c_1, c_2 and c_3, first we show the positiveness of u_2, we set $c_2 = c_2^+ - c_2^-$ with

$$c_2^+(t,x) \;=\; sup\{c_2(t,x), 0\}\ and\ c_2^-(t,x) = inf\{c_2(t,x), 0\}$$

One multiplies the second equation of the system (4) by c_2^- integrates over Ω, we have

$$\begin{aligned} -\frac{1}{2}\tfrac{d}{dt}\left(\int_\Omega \left(c_2^-\right)^2 (t,x)\, dx \right) &= \int_\Omega \left| \beta \nabla c_2^-(t,x) \right|^2 dx + (g+m+k) \int_\Omega \left(c_2^-\right)^2 (t,x)\, dx \\ &\quad - b \int_\Omega c_1 \left(c_2^-\right)^2 (t,x)\, dx + \int_\omega \chi_{\omega_2}(x) \left(v \left(c_2^-\right)^2 \right)(t,x)\, dx \end{aligned}$$

As $c_1 \leq N$ then $-bc_1 \geq -bN$, we have $-\frac{1}{2}\frac{d}{dt}\left(\int_\Omega \left(c_2^-\right)^2(t,x)\,dx\right) \geq -b\int_\Omega N\left(c_2^-\right)^2(t,x)\,dx$. Gronwall's inequality leads to

$$\int_\Omega \left(c_2^-\right)^2(t,x)\,dx \leq e^{tbN}\int_\Omega \left(c_2^-\right)^2(0,x)\,dx$$

Then

$$c_2^- = 0$$

One deduces that $c_2(x,t) \geq 0$, $\forall\,(t,x) \in Q$. In addition, we consider the system

$$\begin{cases} \dfrac{\partial c_1}{\partial t} = \lambda\Delta c_1 + \Lambda - bc_1c_2 - mc_1 - u\chi_{\omega_1}(x)c_1 \\ \\ \dfrac{\partial c_3}{\partial t} = \gamma\Delta c_3 + gc_2 - mc_3 + v\chi_{\omega_2}(x)c_2 + u\chi_{\omega_1}(x)c_1 \end{cases} \tag{15}$$

where

$$\begin{cases} F(c_1,c_3) = \Lambda - bc_1c_2 - mc_1 - u\chi_{\omega_1}(x)c_1 \\ G(c_1,c_3) = gc_2 - mc_3 + v\chi_{\omega_2}(x)c_2 + u\chi_{\omega_1}(x)c_1 \end{cases}$$

It is obvious to see that the functions F and G are continuously differentiable satisfying $F(0,c_3) = \Lambda$ and $G(c_1,0) = gc_2 + v\chi_{\omega_2}(x)c_2 + u\chi_{\omega_1}(x)c_1$ for all $c_1,c_3 \geq 0$. Since initial data of system (4-6) are non-negative, we deduce the positivity of c_1 and c_2 [28]. One deduces that $c_1(x,t) \geq 0$, $c_2(x,t) \geq 0$ and $c_3(x,t) \geq 0\,\forall\,(t,x) \in Q$. □

4. THE EXISTENCE OF THE OPTIMAL SOLUTION

In this section, we will prove the existence of an optimal control for problem (4-6) subject to reaction diffusion system and $(u,v) \in U_{ad}$. The main result of this section is the following.

Theorem 2. *Under the conditions of theorem (1) the optimal control problem (4-6) admits an optimal solution* (c^*,u^*,v^*).

Proof. Let

$$J^* = \inf\{J(c,u,v)\} \tag{16}$$

where $(u,v) \in U_{ad}$ and c is the solution of (4-6).

Obviously $J^*$is finite. Therefore there exists a sequence(c^n,u^n,v^n) with $(u^n,v^n)\in U_{ad}$, $c^n=\left(c_1^n,c_2^n,c_3^n\right)\in W^{1,2}\left([0,T];H(\Omega)\right)$, such that

$$(17)\quad \begin{cases} \dfrac{\partial c_1^n}{\partial t}=\lambda\Delta c_1^n+\Lambda-bc_1^nc_2^n-mc_1^n-u^n\chi_{\omega_1}(x)c_1^n \\ \dfrac{\partial c_2^n}{\partial t}=\beta\Delta c_2^n+bc_1^nc_2^n-(g+m+k)\,c_2^n-v^n\chi_{\omega_2}(x)c_2^n & (t,x)\in Q \\ \dfrac{\partial c_3^n}{\partial t}=\gamma\Delta c_3^n+gc_2^n-mc_3^n+v^n\chi_{\omega_2}(x)c_2^n+u^n\chi_{\omega_1}(x)c_1^n \end{cases}$$

$$(18)\qquad \frac{\partial c_1^n}{\partial\eta}=\frac{\partial c_2^n}{\partial\eta}=\frac{\partial c_3^n}{\partial\eta}=0 \qquad (t,x)\in\Sigma$$

$$(19)\qquad c_i^n(0,x)=c_i^0\ for.i=1,2,3 \qquad x\in\Omega$$

and

$$(20)\qquad J^*\le J\left(c^n,(u^n,v^n)\right)\le J^*+\frac{1}{n} \qquad (\forall n\ge 1)$$

Since $H^1(\Omega)$ is compactly embedded in $L^2(\Omega)$, we infer that $c_1^n(t)$ is compact in $L^2(\Omega)$. Show that $\left\{c_1^n(t),n\ge 1\right\}$ is equicontinuous in $C\left([0,T]:L^2(\Omega)\right)$. As $\dfrac{\partial c_1^n}{\partial t}$ is bounded in $L^2(Q)$, $i=1,2,3$, this implies that for all $s,t\in[0,T]$

$$(21)\qquad \left|\int_\Omega (c_1^n)^2(t,x)\,dx-\int_\Omega (c_1^n)^2(s,x)\,dx\right|\le K|t-s|$$

for any s, $t\in[0,T]$. The Ascoli-Arzela Theorem (See [24]) implies that c_1^n is compact in $C\left([0,T]:L^2(\Omega)\right)$. We conclude that there exist a subsquence denoted again c_1^n such that

$c_1^n\longrightarrow c_1^*$ in $L^2(\Omega)$, uniformly with respect to t.

Analogously $c_i^n\longrightarrow c_i^*$in $L^2(\Omega)$, $i=2,3$ uniformly with respect to t.

The boundedness of Δc_i^n in $L^2(Q)$ implies its weak convergence in $L^2(Q)$ on a subsequence denoted again $\triangle c_i^n$ then for all distribution ψ

$$\int_Q \psi\Delta c_i^n=\int_Q c_i^n\triangle\psi\to\int_Q c_i^*\triangle\psi=\int_Q\psi\Delta c_i^*$$

Which implies that $\Delta c_i^n\rightharpoonup\Delta c_i^*$in $L^2(Q)$ for $i=1,2,3$. Here and everywhere below the sign $\rightharpoonup$ denotes the weak convergence in the specified space. Estimates lead to

$$\frac{\partial c_i^n}{\partial t} \rightharpoonup \frac{\partial c_i^*}{\partial t} \, in \, L^2(Q), i = 1,2,3$$

$$c_i^n \rightharpoonup c_i^* \, in \, L^2\left(0,T : H^2(\Omega)\right), i = 1,2,3$$

$$c_i^n \rightharpoonup c_i^* \, in \, L^\infty\left(0,T : H^1(\Omega)\right), i = 1,2,3$$

Writing $c_1^n c_2^n - c_1^* c_2^* = \left(c_1^n - c_1^*\right) c_2^n + c_1^* \left(c_2^n - c_2^*\right)$ and making use of the convergences $c_i^n \longrightarrow c_i^* \text{in } L^2(Q)$, $i = 1,2$ and of the boundedness of c_1^*, c_2^n in $L^\infty(Q)$, one arrives at $c_1^n c_2^n \mapsto c_1^* c_2^* \text{in } L^2(Q)$. We also have $v^n \rightharpoonup v^*$ and $u^n \rightharpoonup u^* \text{in } L^2(Q)$ on a subsequence denoted again v^n and u^n. Since U_{ad} is a closed and convex set in $L^2(Q)$, it is weakly closed, so $(u^*, v^*) \in U_{ad}$ and as above $u^n \chi_{\omega_1}(x) c_1^n \to \chi_{\omega_1}(x) u^* c_1^*$ in $L^2([0,T] \times \omega)$ also $v^n \chi_{\omega_2}(x) c_2^n \to v^* \chi_{\omega_2}(x) c_2^* \text{in } L^2([0,T] \times \omega)$. Now we may pass to the limit in $L^2(Q)$ as $n \to \infty$ in (17-19) to deduce that $(c^*, (u^*, v^*))$ is an optimal solution. □

5. Necessary Optimality Conditions

In this section, we establish the optimality condition corresponding to problem (1) and we investigate a characterization of optimal control.

Theorem 3. *The mapping $c : U_{ad} \to W^{1,2}([0,T], H(\Omega))$ with $c_i \in L(T,\Omega)$ is Gateaux differentiable with respect to $w^* = \begin{pmatrix} u^* \\ v^* \end{pmatrix}$. For $w = \begin{pmatrix} u \\ v \end{pmatrix} \in U_{ad}$, $c'(w) w^* = C$ is the unique solution in $W^{1,2}([0,T], H(\Omega))$ with $C_i \in L(T,\Omega)$ of the problem*

$$\begin{cases} \dfrac{\partial C}{\partial t} = AC + JC + Gw \text{ sur } Q \\ \\ C(0,x) = 0 \end{cases} \tag{22}$$

with

$$J = \begin{pmatrix} -bc_2^* - m - u^* \chi_{\omega_1}(x) & -bc_1^* & 0 \\ bc_2^* & \beta c_1^* - g - m - k - v^* \chi_{\omega_2}(x) & 0 \\ u^* \chi_{\omega_1}(x) & g + v^* \chi_{\omega_2}(x) & -m \end{pmatrix},$$

$$G=\begin{pmatrix} -c_1^*\chi_{\omega_1}(x) & 0 \\ 0 & -c_2^*\chi_{\omega_2}(x) \\ c_1^*\chi_{\omega_1}(x) & c_2^*\chi_{\omega_2}(x) \end{pmatrix}$$

Proof. In order to establish the result of this theorem, let (c^*,w^*) be an optimal pair and $w^\varepsilon = w^* + \varepsilon w$ $(\varepsilon>0)\in L^2(Q)$. Denote by $c^\varepsilon=\left(c_1^\varepsilon,c_2^\varepsilon,c_3^\varepsilon\right)$ and $c^*=\left(c_1^*,c_2^*,c_3^*\right)$ the solution of (17-19) corresponding to w^ε and w^*, respectively. Put $c_i^\varepsilon = c_i^* + \varepsilon C^\varepsilon$ for $i=1,2,3$

Subtracting system (17-19) corresponding c^* from the system corresponding to c^ε we get

(23)
$$\begin{cases} \frac{\partial C_1^\varepsilon}{\partial t} = \lambda\Delta C_1^\varepsilon + \left(-bc_2^* - m - u^*\chi_{\omega_1}(x)\right)C_1^\varepsilon + \left(-bc_1^*\right)C_2^\varepsilon - u^*\chi_{\omega_1}(x)c_1^* \\ \frac{\partial C_2^\varepsilon}{\partial t} = \beta\Delta C_2^\varepsilon + bc_2^*C_1^\varepsilon + \left(\beta c_1^* - g - m - k - v^*\chi_{\omega_2}(x)\right)C_2^\varepsilon - v^*\chi_{\omega_2}(x)c_2^* \quad (x,t)\in Q=[0,T]\times\Omega \\ \frac{\partial C_3^\varepsilon}{\partial t} = \gamma\Delta C_3^\varepsilon + \left(u^*\chi_{\omega_1}(x)\right)C_1^\varepsilon + \left(g+v^*\chi_{\omega_2}(x)\right)C_2^\varepsilon - mC_3^\varepsilon + u^*\chi_{\omega_1}(x)c_1^* + v^*\chi_{\omega_2}(x)c_2^* \end{cases}$$

(24)
$$\frac{\partial C_1^\varepsilon}{\partial \eta} = \frac{\partial C_2^\varepsilon}{\partial \eta} = \frac{\partial C_3^\varepsilon}{\partial \eta} = 0\,(t,x)\in\Sigma=[0,T]\times\partial\Omega$$

(25)
$$C_i^\varepsilon(0,x)=0\, x\in\Omega,\ for\, i=1,2,3$$

Now we show that C_i^ε are bounded in $L^2(Q)$ uniformly with respect to ε and that c_i^ε in $L^2(Q)$. To this end, denote

$$J^\varepsilon = \begin{pmatrix} -bc_2^\varepsilon - m - u^*\chi_{\omega_1}(x) & -bc_1^* & 0 \\ bc_2^\varepsilon & \beta c_1^* - g - m - k - v^\varepsilon\chi_{\omega_2}(x) & 0 \\ u^\varepsilon\chi_{\omega_1}(x) & g + v^\varepsilon\chi_{\omega_2}(x) & -m \end{pmatrix}$$

and $G=\begin{pmatrix} -c_1^*\chi_{\omega_1}(x) & 0 \\ 0 & -c_2^*\chi_{\omega_2}(x) \\ c_1^*\chi_{\omega_1}(x) & c_2^*\chi_{\omega_2}(x) \end{pmatrix}$

Then the system (23-25) can be written in the form

(26)
$$\begin{cases} \frac{\partial C^\varepsilon}{\partial t} = AC^\varepsilon + J^\varepsilon C^\varepsilon + Gw \text{ on } [0,T] \\ C^\varepsilon(0)=0 \end{cases}$$

We consider $(S(t), t \geq 0)$ the semi-group generated by A, then the solution of system(26) is given by

$$C^{\varepsilon}(t) = \int_0^t S(t-s) J^{\varepsilon}(s) C^{\varepsilon}(s) ds + \int_0^t S(t-s) (Gw)(s) ds, \tag{27}$$

since the elements of the matrix J^{ε} are bounded uniformly with respect to ε, the Gronwall's inequality we guide to

$$\|C_i^{\varepsilon}\|_{L^2(Q)} \leq \Gamma \tag{28}$$

for some constant $\Gamma > 0$ $(i = 1,2,3)$. Then

$$\|c_i^{\varepsilon} - c_i^*\|_{L^2(Q)} = \varepsilon \|C_i^{\varepsilon}\|_{L^2(Q)} \tag{29}$$

Thus $c_i^{\varepsilon} \to c_i^*$in $L^2(Q)$, $i = 1,2,3$. Let

$$J = \begin{pmatrix} -bc_2^* - m - u^* \chi_{\omega_1}(x) & -bc_1^* & 0 \\ bc_2^* & \beta c_1^* - g - m - k - v^* \chi_{\omega_2}(x) & 0 \\ u^* \chi_{\omega_1}(x) & g + v^* \chi_{\omega_2}(x) & -m \end{pmatrix}$$

$$\text{and} \quad G = \begin{pmatrix} -c_1^* \chi_{\omega_1}(x) & 0 \\ 0 & -c_2^* \chi_{\omega_2}(x) \\ c_1^* \chi_{\omega_1}(x) & c_2^* \chi_{\omega_2}(x) \end{pmatrix}$$

Then the system (23-25) can be written as

$$\begin{cases} \frac{\partial C}{\partial t} = AC + JC + Gw \text{ on } [0,T] \\ \\ C(0) = 0 \end{cases} \tag{30}$$

and its solution is given by

$$C(t) = \int_0^t S(t-s) J(s) C(s) ds + \int_0^t S(t-s) (Gw)(s) ds, \tag{31}$$

By (27) and (31) one deduces that

$$C^{\varepsilon}(t) - C(t) = \int_0^t S(t-s) J^{\varepsilon}(s) (C^{\varepsilon} - C) + C(s) (J^{\varepsilon}(s) - J(s)) ds. \tag{32}$$

Since all the elements of the matrix J^{ε}tend to the corresponding elements of the matrix J in $L^2(Q)$, by using the Gronwall's inequality, we derive that Thus $C_i^{\varepsilon} \to C_i^*$in $L^2(Q)$ as $\varepsilon \to 0$, for $i = 1,2,3$. □

Let $p = (p_1, p_2, p_3)$ the adjoint variable, we can write the dual system associated to our problem

$$\begin{cases} -\dfrac{\partial p}{\partial t} - Ap - J^* p = D^* D c^* & t \in [0,T] \\ p(T,x) = 0 \\ \dfrac{\partial p}{\partial \eta} = 0 \end{cases} \tag{33}$$

where w^* is the optimal control, $c^* = \left(c_1^*, c_2^*, c_3^*\right)$ is the optimal state and D is the matrix defined by $D = \begin{pmatrix} 0 & 0 & 0 \\ 0 & 1 & 0 \\ 0 & 0 & -1 \end{pmatrix}$.

Lemma 4. *Under hypotheses of theorem 1, if $(c^*, (u^*, v^*))$ is an optimal pair, then the dual system (33) admits a unique strong solution $p \in W^{1,2}([0,T], H(\Omega))$ with $p_i = (p_1, p_2, p_3) \in L(T, \Omega)$ for $i = 1,2,3$.*

Proof. The lemma can be proved by making the change of variable $s = T - t$ and the change of functions $q_i(s,x) = p_i(T-s,x) = p_i(t,x), (t,x) \in Q$, $i = 1,2,3$. And applying the same method as in the proof above. □

Now, we can find the first order necessary condition by applying standard optimality techniques, analyzing the objective functional and utilizing relationships between the state and adjoint equations [29].

Theorem 5. *Let w^*be an optimal control of (23-25) and let $c^* \in W^{1,2}(0,T;H(\Omega))$ with $c_i^* \in L(T,\Omega)$ for $i = 1,2,3$ be the optimal state, that is c^* is the solution to (1.2) with the control w^*.*

Then, there exists a unique solution $p \in W^{1,2}(0,T,H(\Omega))$ of the linear problem

$$\begin{cases} -\frac{\partial p}{\partial t} - Ap - J^* p = D^* Dc^* & t \in [0,T] \\ p(T,x) = 0 \\ \frac{\partial p}{\partial \eta} = 0 \end{cases} \tag{34}$$

and

(35)
$$u^* = min\left(1, max\left(0, \frac{c_1^* \chi_{\omega_1}(x)}{\rho}(p_1 - p_3)\right)\right) and\, v^* = min\left(1, max\left(0, \frac{c_2^* \chi_{\omega_2}(x)}{\rho}(p_2 - p_3)\right)\right).$$

Proof. Suppose w^* is an optimal control and $c^* = \left(c_1^*, c_2^*, c_3^*\right) = (c_1, c_2, c_3)(w^*)$ are the corresponding state variables. Putting $w^\varepsilon = w^* + \varepsilon h \in U_{ad}, h = \begin{pmatrix} h_1 \\ h_2 \end{pmatrix} \in (L^2(0,T;L^2(\Omega)))^2$ and corresponding state solution $c^\varepsilon = \left(c_1^\varepsilon, c_2^\varepsilon, c_3^\varepsilon\right) = (c_1, c_2, c_3)(w^\varepsilon)$.

Since the minimum of the objective functional is attained at w^*, we have

$$\begin{aligned} J(w^*)(h) &= lim_{\varepsilon \to 0} \frac{1}{\varepsilon}\left(J(w^\varepsilon) - J(w^*)\right) \\ &= lim_{\varepsilon \to 0} \frac{1}{\varepsilon}\Big(\int_0^T \int_\Omega (c_2^\varepsilon)^2 - (c_2^*)^2 dxdt - \int_0^T \int_\Omega (c_3^\varepsilon)^2 - (c_3^*)^2 dxdt \\ &+ \rho \int_0^T \int_\Omega (u^\varepsilon)^2 - (u^*)^2 dxdt + \rho \int_0^T \int_\Omega (v^\varepsilon)^2 - (v^*)^2 dxdt\Big) \\ &= lim_{\varepsilon \to 0}\Big(\int_0^T \int_\Omega \left(\frac{c_2^\varepsilon - c_2^*}{\varepsilon}\right)(c_2^\varepsilon + c_2^*) dxdt - \int_0^T \int_\Omega \left(\frac{c_3^\varepsilon - c_3^\varepsilon}{\varepsilon}\right)(c_3^\varepsilon + c_3^*) dxdt \\ &+ \rho \int_0^T \int_\Omega (\varepsilon h_1)^2 + 2h_1 u^* dxdt + \rho \int_0^T \int_\Omega (\varepsilon h_2)^2 + 2h_2 v^* dxdt\Big) \end{aligned}$$

as $lim_{\varepsilon \to 0} \frac{c_2^\varepsilon - c_2^*}{\varepsilon} = lim_{\varepsilon \to 0} \frac{c_2(w^* + \varepsilon h) - c_2^*}{\varepsilon} = c_2'(w^*)h,\ c_2^\varepsilon \longrightarrow c_2^* in L^2(Q) and\, c_2^\varepsilon, c_2^* \in L^\infty(Q), same\, for\, c_3^\varepsilon$.

Then we obtain

$$\begin{aligned} J(w^*)(h) &= 2\int_0^T \int_\Omega (c_2^* - c_3^*) c'(w^*) h\, dxdt + 2\rho \int_0^T \int_\Omega h_1 u^* dxdt + 2\rho \int_0^T \int_\Omega h_2 v^* dxdt \\ &= 2\int_0^T \langle Dc^*, DC\rangle_{H(\Omega)} + 2\rho \int_0^T \langle w^*, h\rangle_{(L^2(\Omega))^2} dt \end{aligned}$$

Since J is Gateaux differentiable at w^* and U_{ad} is convex, it is seen that $J'(w^*)(z - w^*) \geq 0$ for all $z \in U_{ad}$

$$J^{'}(w^*)(z-w^*) = 2\int_0^T \langle Dc^*, DC\rangle_{H(\Omega)} + 2\rho \int_0^T \langle w^*, z-w^*\rangle_{L^2(\Omega)}\, dt$$

We have

$$\begin{aligned}
\int_0^T \langle Dc^*, DC\rangle_{H(\Omega)} &= \int_0^T \langle D^*Dc^*, C\rangle_{H(\Omega)}\, dt \\
&= \int_0^T \left\langle -\frac{\partial p}{\partial t} - Ap - Jp, C \right\rangle_{H(\Omega)} dt \\
&= \int_0^T \left\langle P, \frac{\partial C}{\partial t} - AC - JC \right\rangle_{H(\Omega)} dt \\
&= \int_0^T \langle P, G(z-w^*)\rangle_{H(\Omega)}\, dt \\
&= \int_0^T \langle G^*P, (z-w^*)\rangle_{(L^2(\Omega))^2}\, dt
\end{aligned}$$

We deduce that $J^{'}(w^*)(z-w^*) \geq 0$ for all $z \in U_{ad}$ equivalent to $\int_0^T \langle G^*P, (z-w^*)\rangle_{(L^2(\Omega))^2}\, dt \geq 0$ for all $z \in U_{ad}$. By standard arguments varying z, we get

$$w^* = -\frac{1}{\rho} G^*P$$

Afterwards

$$u^* = \frac{c_1^*\chi_{\omega_1}(x)}{\rho}(p_1 - p_3) \; and \; v^* = \frac{c_2^*\chi_{\omega_2}(x)}{\rho}(p_2 - p_3)$$

As $(u^*, v^*) \in U_{ad}$, we have

$$u^* = min\left(1, max\left(0, \frac{c_1^*\chi_{\omega_1}(x)}{\rho}(p_1 - p_3)\right)\right) and\, v^* = min\left(1, max\left(0, \frac{c_2^*\chi_{\omega_2}(x)}{\rho}(p_2 - p_3)\right)\right)$$

□

6. NUMERICAL SIMULATIONS

In this section, we present the numerical results that illustrate and reinforce the effect of our control strategy. This strategy consists of applying two terms of control, representing the vaccination and the treatment program, in order to fight against the spread of the COVID-19 disease. We developed a code in MATLAB and simulated our results using different data. Regarding the numerical method, we give numerical simulations of our optimality system, which is formulated by state equations with initial conditions and boundary conditions (4-6),

adjoint equations with transversality conditions, and a characterization of the optimal control. We apply the forward-backward sweep method (FBSM) [30] to solve our optimality system in an iterative process. The state equations are solved using a direct method in time by employing Euler explicit method, in order to discretize the second order derivatives $\triangle S_T$, $\triangle I_T$, and $\triangle R_T$ we use the second order Euler explicit method, initial control variables are guessed in the beginning of the iterative method, next, the adjoint equations are solved backward in time. Finally, the control variables are updated with the current state and adjoint solutions. The iterative process is repeated until reaching a tolerance criterion.

To show the importance of our work, and without loss of generality, we consider a $40km \times 30km$ rectangular grid denoted. We assume that the susceptible individuals are homogeneously distributed, with 45 in each $1km \times 1km$ subdomain, except in the subdomain $\Omega_1 = cell(20;15)$, when the disease starts at the middle of Ω ; where we introduce 5 infectious, and keep 40 susceptible. All simulations are performed using the parameter values in Table 1. For all figures below, the red part of the colored bars contains a very large number of individuals, while the blue part contains the smaller numbers.

In Fig.1 (a), Fig.1 (b) and Fig.1 (c), we present simulations illustrating the dynamics of susceptible, infected and cured individuals in the case where no control strategy is yet proposed (see differential system (1). We note that in all these figures presented here, the simulations give us an idea of the spread of the disease in the case where the infection starts in the middle, in order to show the effect of the spatial factor, and the contribution of mobility in the transmission of Covid-19.

TABLE 1. Initial conditions and parameters values

Parameter	Value	Description
S_0	$45\,for\,\Omega_j$ $40\,for\,\Omega_1$	Initial susceptible population
I_0	$0\,for\,\Omega_j$ $5\,for\,\Omega_1$	Initial infected population
R_0	0	Initial immune population
k	0.01	Mortality due to infection
d	0.02	Natural mortality rate
b	0.24	Transmission rate
g	0.02	Recovery rate
Λ	0.01	birth rate
$\lambda, \beta, \gamma = 1, 2, 3$	0.6	Diffusion coefficient

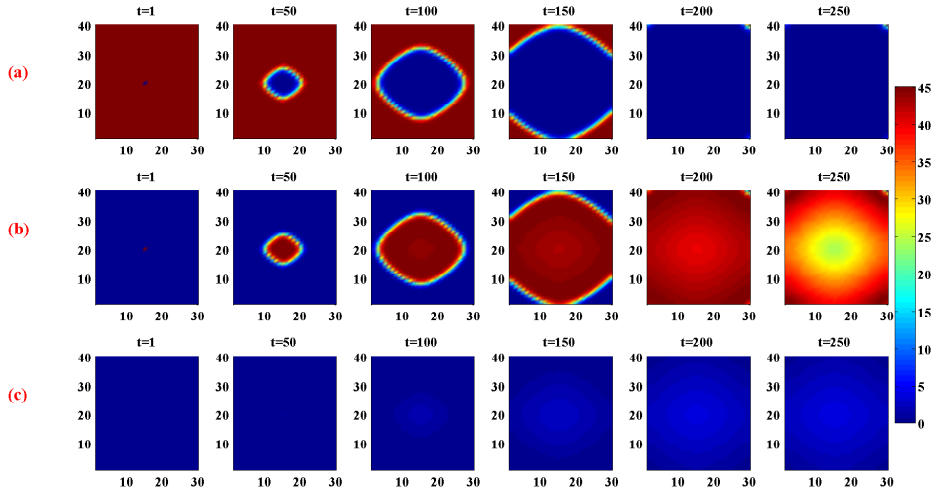

FIGURE 1. States of system without controls. (a) Susceptibles behavior in the absence of control. (b) Infectives behavior in the absence of control. (c) Removed behavior in the absence of control

We can see more clearly that the number of susceptible individuals has decreased, and the disease is spreading rapidly to reach the whole population, which indicates the danger of the disease. Regarding the class of cured individuals, there are a few cured individuals (about 5 persons). These remarks observed in the simulations lead us to consider the definition of an appropriate control strategy.

As a demonstration and clarification of the utility of our Covid-19 transmission control strategy, we present a regional control aimed at preserving a specific region from the impact of Covid-19 transmission from neighboring regions. We consider two treatment areas as a rectangle $\omega_1 = [20,30] \times [0,15]$ at the border, and $\omega_2 = [10,20] \times [15,25]$ in the center. This strategy consists of the introduction of two controls, the first being vaccination to slow the spread of infection and the second being integrated treatment to reduce actively infected individuals. The main objective is to show the effectiveness of our vaccination and treatment procedures in controlling the spread of Covid-19 virus disease in two different regions; the assumption is that a patient is treated in a region $\omega_i, i = 1,2$ immediately after infection with Covid-19 virus.

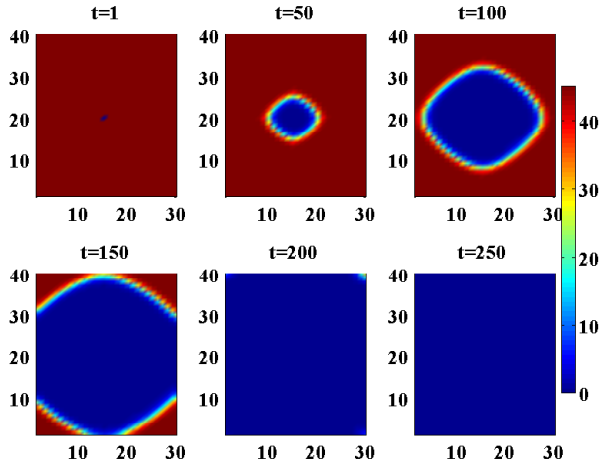

FIGURE 2. Susceptible behavior within Ω with control in regions ω_1 and ω_2.

Once our spatio-temporal control strategy based on vaccination and treatment is introduced, we can clearly infer its effect in slowing the spread of infection in the ω_i, $i = 1,2$ areas. Specifically, in Figure 3, after $t = 250$, the density of infected people decreases from 30

individuals per cell (in the absence of control) to 0 individuals per cell (in the presence of control treatment) in the ω_i, $i = 1,2$ zones, while there is no changes outside ω_i, $i = 1,2$ where the number of infected remains the same (see Figs. 3, 4).

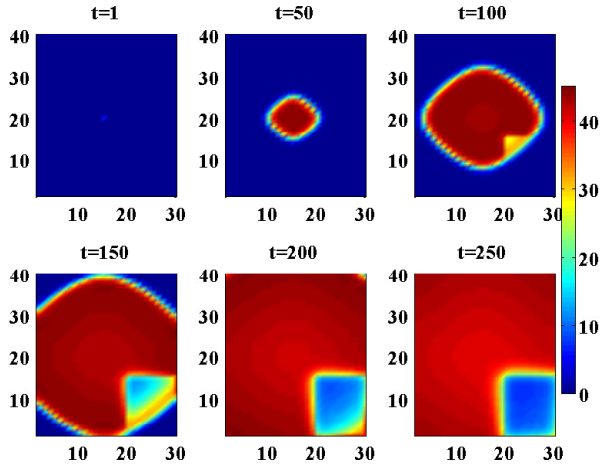

FIGURE 3. Infected behavior within Ω with control in region ω_1.

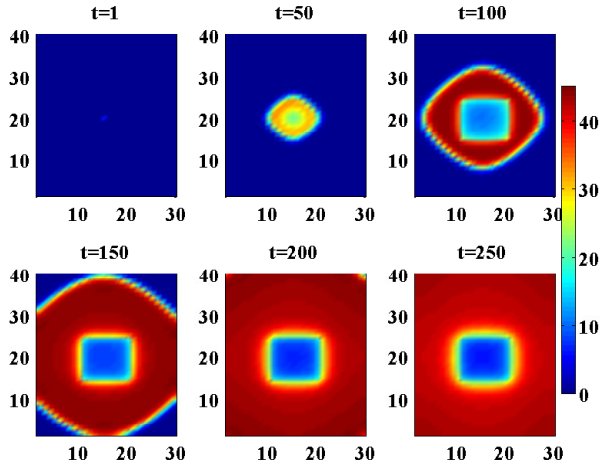

FIGURE 4. Infected behavior within Ω with control in region ω_2.

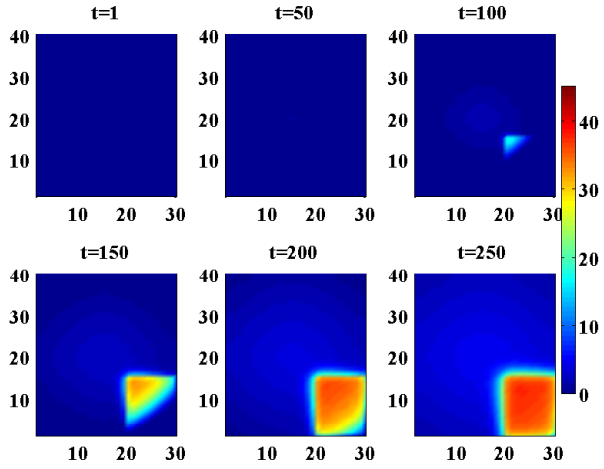

FIGURE 5. Recovered behavior within Ω with control in region ω_1.

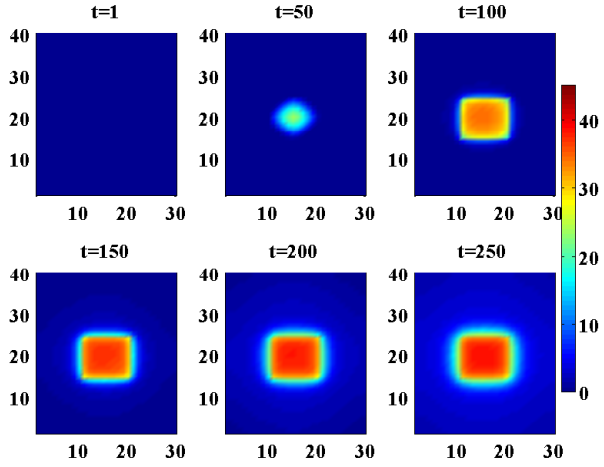

FIGURE 6. Recovered behavior within Ω with control in region ω_2.

Finally, as a comparison of the behavior of the susceptible population, Figs. 1 and 2 show the disappearance of this group in the absence and presence of control. But the difference of these two cases, is the epidemiological movement of susceptible individuals, in the first case, susceptible individuals are transferred to the infected class, as it is shown in Fig1(a) and Fig1(b), but in the second case, susceptible individuals are transferred to the removed class in the areas targeted, while there is no change outside these areas, as it is shown in Figs. 5 and 6. Which

is very advantageous and reflects the importance of our regional control strategy in the fight against the spread of Covid-19 in specific areas, as it can be seen in Figs. 5 and 6.

7. Conclusion

In this article, we present an interesting application theory to study the optimal combination of vaccination and treatment strategies for spatiotemporal epidemic models described by a system of partial differential equations. The control variable is the spatial and temporal distribution of the vaccine and treatment. The existence of solutions to the state system and the existence of optimal controls have been proved. For our given functional objective, optimal control is characterized in terms of the corresponding state and adjoint functions. A numerical simulation is executed, showing that optimal control of treatment time is very efficacious in reducing the total number of infections for diverse scripts of COVID-19.

Data Availability

The disciplinary data used to support the fndings of this study have been deposited in the Network Repository (http://www.networkrepository.com).

Conflict of Interests

The authors declare that there is no conflict of interests.

References

[1] D. Bernoulli, Essai d'une nouvelle analyse de la mortalité causée par la petite verole et des avantages de l'inoculation pour la prevenir. Mem. Math. Phys. Acad. Roy. Sci., Paris, 1–45. In Histoire de l'Academie Royale des Sciences, (1766).

[2] K. Dietz, J.A.P. Heesterbeek, Daniel Bernoulli's epidemiological model revisited, Math. Biosci. 180 (2002), 1–21. https://doi.org/10.1016/s0025-5564(02)00122-0.

[3] R. Ross, The prevention of Malaria, John Murray, London, (1911).

[4] W.O. Kermack, A.G. McKendrick, A contribution to the mathematical theory of epidemics, Proc. R. Soc. Lond. A. 115 (1927), 700–721. https://doi.org/10.1098/rspa.1927.0118.

[5] C. Ji, D. Jiang, N. Shi, The behavior of an sir epidemic model with stochastic perturbation, Stoch. Anal. Appl. 30 (2012), 755–773. https://doi.org/10.1080/07362994.2012.684319.

[6] Yu.A. Kuznetsov, C. Piccardi, Bifurcation analysis of periodic SEIR and SIR epidemic models, J. Math. Biol. 32 (1994), 109–121. https://doi.org/10.1007/bf00163027.

[7] C.C. McCluskey, Complete global stability for an SIR epidemic model with delay - Distributed or discrete, Nonlinear Anal.: Real World Appl. 11 (2010), 55–59. https://doi.org/10.1016/j.nonrwa.2008.10.014.

[8] S. Pathak, A. Maiti, G.P. Samanta, Rich dynamics of an SIR epidemic model, Nonlinear Anal.: Model. Control. 15 (2010), 71–81. https://doi.org/10.15388/na.2010.15.1.14365.

[9] R. Miller Neilan, S. Lenhart, Optimal vaccine distribution in a spatiotemporal epidemic model with an application to rabies and raccoons, J. Math. Anal. Appl. 378 (2011), 603–619. https://doi.org/10.1016/j.jmaa.2010.12.035.

[10] G. Saccomandi, The spatial diffusion of diseases, Math. Computer Model. 25 (1997), 83–95. https://doi.org/10.1016/s0895-7177(97)00096-4.

[11] M.V. Reyes, The disproportional impact of COVID-19 on African Americans, Health Human Rights J. 22 (2020), 299–307.

[12] University-Based Institute for Advanced Studies (UBIAS), Essays on the post-COVID-19 world, http://www.ubias.net/essays-covid19.

[13] J. Thomas, A short note on COVID 19, Arch. Med. 16 (2020), 4.

[14] https://www.who.int/emergencies/diseases/novel-coronavirus-2019.

[15] J. Arino, R. Jordan, P. van den Driessche, Quarantine in a multi-species epidemic model with spatial dynamics, Math. Biosci. 206 (2007), 46–60. https://doi.org/10.1016/j.mbs.2005.09.002.

[16] E. Zerrik, A. Boutoulout, A.E. Jai, Actuators and regional boundary controllability of parabolic systems, Int. J. Syst. Sci. 31 (2000), 73–82. https://doi.org/10.1080/002077200291479.

[17] S.B. Rhila, M. Rachik, Optimal control problem of a tuberculosis model with spatial dynamics, Commun. Math. Biol. Neurosci. 2020 (2020), 26. https://doi.org/10.28919/cmbn/4438.

[18] T.K. Kar, A. Batabyal, Stability analysis and optimal control of an SIR epidemic model with vaccination, Biosystems. 104 (2011), 127–135. https://doi.org/10.1016/j.biosystems.2011.02.001.

[19] H. Laarabi, E.H. Labriji, M. Rachik, A. Kaddar, Optimal control of an epidemic model with a saturated incidence rate, Nonlinear Anal.: Model. Control. 17 (2012), 448–459. https://doi.org/10.15388/na.17.4.14050.

[20] K.S. Lee, A.A. Lashari, Stability analysis and optimal control of pine wilt disease with horizontal transmission in vector population, Appl. Math. Comput. 226 (2014), 793–804. https://doi.org/10.1016/j.amc.2013.09.061.

[21] G. Zaman, Y.H. Kang, I.H. Jung, Optimal treatment of an SIR epidemic model with time delay, Biosystems. 98 (2009), 43–50. https://doi.org/10.1016/j.biosystems.2009.05.006.

[22] N.J. Sullivan, A. Sanchez, P.E. Rollin, et al. Development of a preventive vaccine for Ebola virus infection in primates, Nature. 408 (2000), 605–609. https://doi.org/10.1038/35046108.

[23] L.N. Guin, P.K. Mandal, Spatiotemporal dynamics of reaction–diffusion models of interacting populations, Appl. Math. Model. 38 (2014), 4417–4427. https://doi.org/10.1016/j.apm.2014.02.022.

[24] H. Brezis, Functional analysis, Sobolev spaces and partial differential equations, Springer New York, 2011. https://doi.org/10.1007/978-0-387-70914-7.

[25] I.I. Vrabie, C_0-semigroups and applications, Volume 191 of North-Holland Mathematics Studies, Elsevier, Amsterdam, (2003).

[26] V. Barbu, Mathematical methods in optimization of differential systems, Volume 310, Springer, Dordrecht, (2012).

[27] A. Pazy, Semigroups of linear operators and applications to partial differential equations, Volume 44, Springer, New York, (2012).

[28] J. Smoller, Shock waves and reaction–diffusion equations, Volume 258, Springer, New York, (2012).

[29] L.S. Pontryagin, V.G. Boltyanskii, R.V. Gamkrelidze, et al. The mathematical theory of optimal processes, International series of monographs in pure and applied mathematics, Interscience, New York, (1962).

[30] M. McAsey, L. Mou, W. Han, Convergence of the forward-backward sweep method in optimal control, Comput. Optim. Appl. 53 (2012), 207–226. https://doi.org/10.1007/s10589-011-9454-7.